Effect of oxygen stoichiometry on spin, charge, and orbital ordering in manganites

R. Vidya,* P. Ravindran, P. Vajeeston, A. Kjekshus, and H. Fjellvåg
Department of Chemistry, University of Oslo, P.O. Box 1033 Blindern, N-0315 Oslo, Norway
(Received 8 September 2003; published 18 March 2004)

Using full-potential density-functional calculations we show that oxygen stoichiometry plays an important role on spin, charge, and orbital ordering in manganites. The electronic structure and magnetic properties of $LaBaMn_2O_{5+\delta}$ have been studied for $\delta=0$, 0.5, and 1; for $\delta=0$ and 0.5 the system exhibits charge, orbital, and antiferromagnetic spin ordering, whereas at $\delta=1$ the charge and orbital orderings disappear but the spin ordering remains. We also bring out an insulator-to-metal transition upon going from $\delta=0$ to 1. The study suggests that one can manipulate the charge and orbital orderings in certain perovskite-like oxides by merely varying the oxygen stoichiometry and hence design oxides with desired electrical and magnetic properties.

DOI: 10.1103/PhysRevB.69.092405 PACS number(s): 71.15.Nc, 71.20.−b, 81.05.Je, 81.40.Rs

There has been an upsurge of interest in perovskite-like manganese-based oxides since the discovery of colossal magnetoresistance (CMR). The CMR manganites display a fascinating diversity of behaviors including several forms of spin, charge, and orbital orderings (hereafter SO, CO, and OO).[1] The electronic, magnetic, and CMR features of a given material are largely determined by the chemical composition and crystal structure and these properties may be quite sensitive to even tiny changes in the atomic architecture. Hence an improved understanding of how composition and structure affect transport and magnetism and this may guide the search for new CMR materials.[2]

The interplay between the crystal symmetry and the atomic orbitals plays a crucial role in the conductivity of the e_g electrons in manganites. The transfer integral (t) of e_g electrons between neighboring Mn sites is mediated by the O-2p orbitals and hence depends on the degree of hybridization between Mn-3d and O-2p orbitals. The substitution of divalent cations on the A site of $REMnO_3$ (RE stands for rare earth) perovskites (e.g., the parent CMR material $LaMnO_3$) induces holes in the e_g band. Many studies have addressed the effect of A-site-substituted cations on SO, CO, and OO. Although it is well known that the long-range CO and the transfer efficiency of CMR materials are very sensitive to the oxygen stoichiometry, a complete picture of the role of the oxygen content and localization is lacking. In an attempt to partly remedy this situation we have studied the SO, CO, and OO in the model system $LaBaMn_2O_{5+\delta}$ ($\delta=0$, 0.5, and 1). In addition to a significant CMR effect, ferromagnetic ordering (viz., T_C) close to room temperature is considered essential for technological applications of manganites. Ba-substituted $LaMnO_3$ offers interesting features[3] with T_C near room temperature and large resistance changes just above [e.g., $T_C \approx 362$ K (Ref. 4) for $La_{0.65}Ba_{0.35}MnO_3$]. Hence the studies on $LaBaMn_2O_{5+\delta}$ may prove to be of basic as well as applied scientific interest.

$LaBaMn_2O_5$ crystallizes in the tetragonal double-perovskite-type structure[3] [space group $P4/nmm$, see Fig. 1(a)]. It consists of double layers of apex-sharing MnO_5 pyramids interleaved by oxygen-empty layers (Ba^{2+} are in the oxygen-apical layers and La^{3+} in the oxygen-empty layers). The Mn-O distances in the polyhedra are influenced by the size difference between La^{3+} and Ba^{2+} owing to their arrangement along c. Two crystallographic types of Mn and O atoms are present and reflected in different O-Mn-O angles (apical=161°; equatorial=180°). $LaBaMn_2O_{5.5}$ is orthorhombic[5] [space group $Ammm$; see Fig. 1(c)]. The additional oxygen atoms for $\delta=0.5$ are at the oxygen-empty layers of the $LaBaMn_2O_5$-type variant. Hence $LaBaMn_2O_{5.5}$ has square pyramidal [around Mn(1)] as well as octahedral [around Mn(2)] coordinations of Mn. $LaBaMn_2O_6$ also has a tetragonal structure[3] [space group $P4/mmm$; see Fig. 1(e)]. The added oxygen atoms complete the conversion from square pyramidal coordination around Mn(1) at $\delta=0$ to octahedral at $\delta=1$. The interesting aspect of $LaBaMn_2O_{5+\delta}$ is that the arrangement of La^{3+} and Ba^{2+} remains unchanged, hence the similarity between the three structures is reinforced.

We have calculated the total energy of $LaBaMn_2O_{5+\delta}$ in the para- (P), ferro- (F), and antiferromagnetic (AF) configurations for the experimentally reported structural parameters. The full-potential linear muffin-tin orbital (FPLMTO) calculations[6] presented in this paper are all-electron, and no shape approximation to the charge density or potential has been used. The basis set is comprised of augmented linear muffin-tin orbitals.[7] The calculations are based on the generalized-gradient-corrected (GGA) density-functional theory as proposed by Perdew *et al.*[8] Spin-orbit coupling is included directly in the Hamiltonian matrix elements for the part inside the muffin-tin spheres. We used a multibasis in order to ensure a well-converged wave function, i.e., several Hankel or Neumann functions, each attached to its own radial function, have been used. Hence the basis included are 6s, 6p, 5p, 5d, and 4f orbitals for La and Ba, 4s, 4p, and 3d orbitals for Mn, and 2s, 2p, and 3d orbitals for O. The spherical-harmonic expansion of the charge density, potential and basis functions was performed up to $\ell_{max}=6$. For the total-energy study the **k**-space integration is done using the special point method with 192 **k** points in the irreducible part of the first Brillouin zone. For the F and AF calculations, the magnetization axes are chosen in accordance with experimental findings.[3,5] In the AF calculation for $LaBaMn_2O_{5.5}$, an explicit supercell with 38 atoms is considered. In order to verify the results obtained from the FPLMTO method and to calculate the occupation matrix of each of the Mn-3d orbitals, we have done similar calculations by the full-potential linearized-augmented plane-wave (FPLAPW) method as implemented in WIEN97.[9] Atomic-sphere radii of 2.8 a.u.

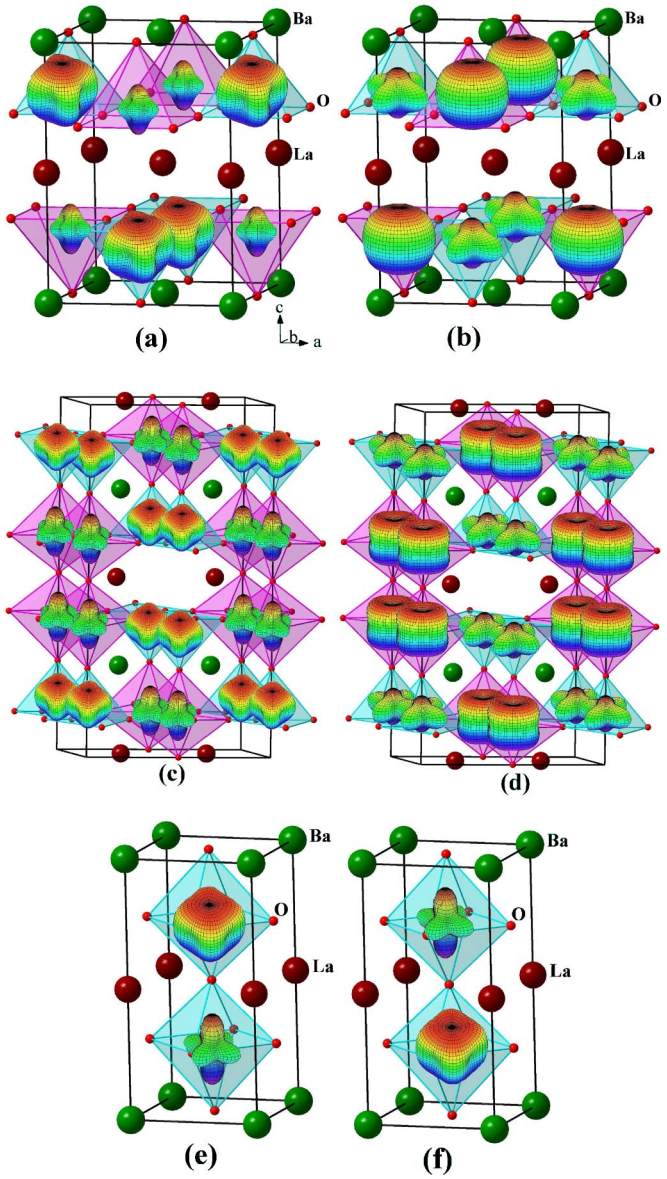

FIG. 1. (Color online) The majority- and minority-spin Mn-3d-electron distribution in (a,b) $LaBaMn_2O_5$, (c,d) $LaBaMn_2O_{5.5}$, and (e,f) $LaBaMn_2O_6$. Atoms inside cyan-colored square pyramids correspond to Mn(1) (Mn in e,f) and those inside pink-colored square pyramids/octahedra correspond to Mn(2).

for La and Ba and 2.0 and 1.6 a.u. for Mn and O, respectively, were used. Exchange and correlation effects are treated using the GGA.[8] The charge densities and potentials in the atomic spheres were represented by spherical harmonics up to $\ell = 6$, whereas in the interstitial region these quantities were expanded in a Fourier series. The radial basis functions of each LAPW were calculated up to $\ell = 10$ and the nonspherical potential contribution to the Hamiltonian matrix had an upper limit of $\ell = 4$. From the ℓ, m projected charge density the CO and OO ordering in these materials are analyzed. For further computational details see Ref. 10.

In $RE_{1-x}AE_xMnO_3$ (AE stands for alkaline earth) compounds the one-electron bandwidth (W) of the Mn-d electrons decreases with decreasing size of the A-site cation, and leads in turn to CO and/or OO. In addition, the A-site substitution changes the valence of the Mn ions. Similarly the variation of the oxygen stoichiometry modifies W and the valence of the Mn ions and this may be used to manipulate SO, CO, and OO in perovskite-like oxides as shown here for the $LaBaMn_2O_{5+\delta}$ phase.

Table I shows the results of FPLMTO calculations performed for the P, F, and AF configurations of $LaBaMn_2O_{5+\delta}$ (similar results were obtained from the FPLAPW method). For all three compositions the AF state is found to have the lowest energy. Table II shows that AF $LaBaMn_2O_5$ has a finite total moment of $0.97\,\mu_B$, implying that it is in fact ferrimagnetic (Ferri). The Ferri ground state and the calculated magnetic moment are in good agreement with the experimental findings.[3] From the difference in the ionic size and magnetic moment, it is experimentally established that Mn(1) corresponds to Mn^{3+} and Mn(2) to Mn^{2+} both in high spin (HS) states. This picture for $LaBaMn_2O_5$ agrees fully with the outcome of the present calculations. In order to analyze changes in the electronic structure with respect to the oxygen stoichiometry, the density of states (DOS) in the ground-state configurations of $LaBaMn_2O_{5+\delta}$ is given in Fig. 2. An energy gap (E_g) of ca. 0.84 eV opens up between the valence and conduction bands in $LaBaMn_2O_5$ [Fig. 2(a)], giving an insulating state in accordance with the experiments. The Ferri ordering leads to significant topological differences in the up- and down-spin DOS.

In general, local-density approximation including Coulomb correlations effects (LDA+U) calculations[11] are thought to be necessary to study the electronic and magnetic properties of transition-metal oxides. However, our calculations show that the insulating behavior and magnetic properties are correctly reproduced by the usual density-functional calculations for the manganites considered in the present study.

As mentioned, t depends on the degree of the hybridization between the Mn-3d and O-2p orbitals, which in turn makes this parameter sensitive to the oxygen stoichiometry. The Jahn-Teller (JT) distortion (associated with HS Mn^{3+}) induces an anisotropy in the interaction between Mn-d and O-p orbitals. Moreover, owing to the size difference between La^{3+} and Ba^{2+} and the oxygen vacancies in the La^{3+} layer, the degree of hybridization between the Mn-d and O-p orbitals is reduced. Hence t and consequently W also decrease. Moreover, the differences in Mn-O-Mn bond angles and Mn-O bond lengths promote significant distinctions between t within and perpendicular to the basal plane of $LaBaMn_2O_5$. The decreases in t and W reduce the double-exchange (DE) interaction, and hence the superexchange interaction overcomes the DE, thus favoring the insulating AF/Ferri CO and/or OO state. Therefore, in addition to Ferri SO, CO occurs with the equal amounts of Mn^{3+} and Mn^{2+} in $LaBaMn_2O_5$. In order to elucidate the effect of oxygen stoichiometry on CO and OO, we show the spatial 3d-electron distribution at each Mn site for the majority and minority spins in Figs. 1(a) and 1(b). The appreciable difference in the distribution of majority and minority d electrons between Mn^{3+} and Mn^{2+} in $LaBaMn_2O_5$, implies the presence of CO.

TABLE I. Total energy (relative to the lowest-energy state in meV/f.u.) in $LaBaMn_2O_{5+\delta}$ for the P, F, and AF phases using FPLMTO with GGA and spin-orbit coupling included.

Composition	P	F	AF
$LaBaMn_2O_5$	3922	438	0
$LaBaMn_2O_{5.5}$	3850	593	0
$LaBaMn_2O_6$	2625	6	0

It is well established that OO plays a crucial role in the magnetic and electronic properties of manganites. As electrons closer to the Fermi level (E_F) participate more in hopping interaction and determine the electronic properties, we show the orbital distribution of such electrons for $LaBaMn_2O_5$ in Fig. 3(a). Owing to the Mn-O-Mn bond angle of 161° for Mn(1), the transfer of the $3d$ electrons is not complete and these electrons therefore tend to localize in a certain pattern over the Mn sites of $LaBaMn_2O_5$. According to the orbital-projected DOS, the d_{xy}, d_{xz}, and d_{yz} orbitals of Mn^{3+} and the $d_{x^2-y^2}$ orbital of Mn^{2+} are found in the energy range -1 eV to E_F, leading to the ordering of these orbitals as shown in Fig. 3(a).

For $LaBaMn_2O_{5.5}$, the ground-state SO is found to be AF, in perfect agreement with the experimental findings.[5] Further, the Mn atoms in the square pyramidal and octahedral coordinations take a HS Mn^{3+} state. The system remains insulating on going to $LaBaMn_2O_{5.5}$, but E_g is reduced to 0.26 eV [Fig. 2(b)]. As half of the square pyramids at $\delta=0$ has been converted into octahedra at $\delta=0.5$, half of the O vacancies in the La layers is filled, and the overlap interaction between Mn-d and O-p orbitals is thereby increased. The bandwidth in turn increases, reducing the band gap. The difference in the crystal fields of square pyramids and octahedra and the accompanied JT distortion increase the carrier-to-lattice coupling and result in localization of charges. Figures 1(c) and 1(d) illustrate the difference in the distribution of majority and minority d electrons between the Mn ions at $\delta=0.5$, indicating the presence of CO. As the orbital degeneracy is lifted due to the JT effect, and anisotropy in the electron-transfer interaction results due to the partial stuffing of the oxygen vacancies, OO occurs. The square pyramidal Mn of $LaBaMn_2O_{5.5}$ have $d_{x^2-y^2}$ and d_{z^2} orbitals near E_F, whereas the octahedral Mn have only $d_{x^2-y^2}$ in the vicinity of E_F. Therefore these orbitals localize to form an OO pattern as shown in Fig. 3(b).

TABLE II. Calculated magnetic moment (in μ_B per Mn atom) for $LaBaMn_2O_{5+\delta}$ in the AF ground state. Total refers to the total magnetic moment per formula unit.

	AF			Experimental		
Composition	Mn(1)	Mn(2)	Total	Mn(1)	Mn(2)	Total
$LaBaMn_2O_5$	3.13	3.99	0.97	2.71[a]	3.21	0.70
$LaBaMn_2O_{5.5}$	3.30	3.34	0.0	3.03[b]	3.43	
$LaBaMn_2O_6$	2.98		0.0	3.50[a]		

[a]Low-temperature neutron-diffraction data, Ref. 3.
[b]Low-temperature neutron-diffraction data, Ref. 5.

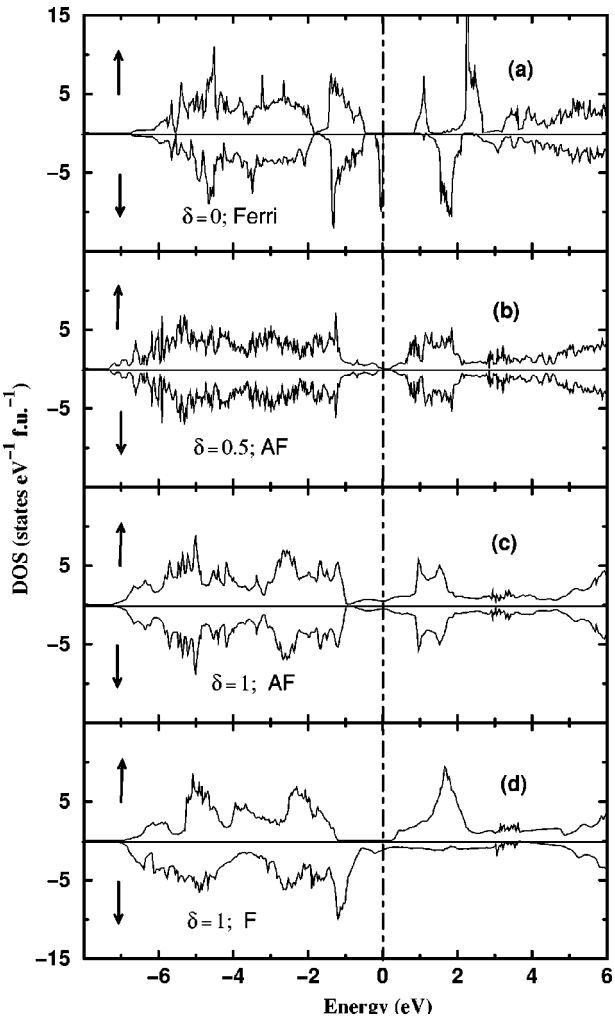

FIG. 2. Total DOS of $LaBaMn_2O_{5+\delta}$ in the magnetic configurations denoted on the illustration. The Fermi level is marked with the dotted line.

Experimentally, F ordering is found[5] for $LaBaMn_2O_6$, whereas our (FPLMTO and FPLAPW) calculations give AF as the ground state. However, recent experimental studies conclude that both F and CE-type AF ordering coexist in $LaBaMn_2O_6$ below 150 K.[12] Moreover, as the calculated energy difference between the F and AF states of $LaBaMn_2O_6$ is very small, a little perturbation may flip the spin arrangement either to F or AF. Hence the coexistence of F and AF states must be considered as a viable outcome. $LaBaMn_2O_6$ contains only one crystallographic type of Mn with an average valence state between 3+ and 4+. The Mn-d exchange splitting is found to be around 3.3, 3.0, and 2.5 eV for $LaBaMn_2O_5$, $LaBaMn_2O_{5.5}$, and $LaBaMn_2O_6$, respectively. The systematic decrease appears to reflect the increasing Mn-d and O-p hybridization interaction and the reduction in magnetic moment of Mn due to increase in its valence state, in the said sequence.

As the oxygen vacancies are filled to the $\delta=1$ limit, the electron bands are broadened and more overlap between the Mn-d and O-p bands is seen. Moreover, the small energy difference between the F and AF states implies that the DE

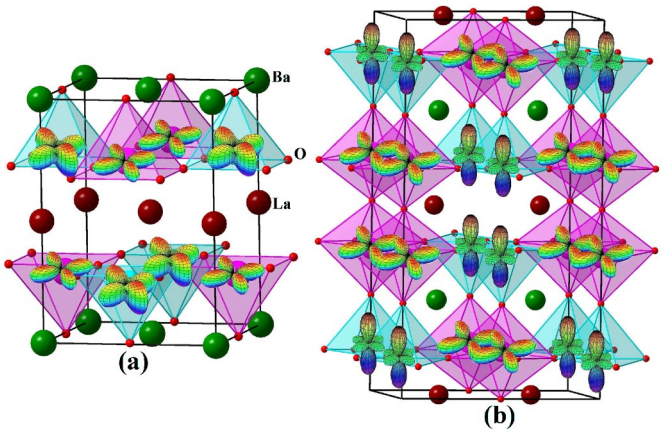

FIG. 3. (Color online) Orbital ordering in (a) $LaBaMn_2O_5$ and (b) $LaBaMn_2O_{5.5}$.

interaction increases (compared with the $\delta=0$ and 0.5 cases), again a consequence of the increased hybridization interaction. Hence the CO state disappears and metallicity appears in $LaBaMn_2O_6$ in accordance with the experimental findings.[3] The metallic behavior of $LaBaMn_2O_6$ can be seen from the small, but finite number of states in DOS at E_F [Fig. 2(c)]. The similarly shaped *d*-electron distributions [see Figs. 1(e) and 1(f)] on the Mn ions also indicate that CO and OO are absent in $LaBaMn_2O_6$.

All three compositions exhibit half-metallicity in the F state (HMF), (with E_g of 2.2, 1.92, and 1.45 eV in the minority-spin channel for $\delta=0$, 0.5, and 1, respectively). The HMF state of $LaBaMn_2O_6$ gains more importance owing to the small energy difference between the F and AF states, which may enable easier conversion from metallic AF to HMF [Fig. 2(d)]. In addition to exchange splitting, the JT distortion as in $LaMnO_3$[13] may play an important role for the occurrence of the HMF in $LaBaMn_2O_6$.

In DE systems, insulator to metal transitions accompanied by disappearance of CO and/or OO due to increased *W* can be achieved by application of external field or pressure. *Since the band characteristics t and W, as well as the valence state of Mn change more drastically with the oxygen contents than by A-site cation substitution in* $(RE,AE)MnO_3$, *one can tune an insulator-to-metal transition from the AF or Ferri CO and/or OO state to a metallic F state by merely varying the oxygen stoichiometry.* Practice has shown that such a conversion may be accompanied by resistivity changes of several orders of magnitude (the CMR effect).

In conclusion, variations in the spin, charge, and orbital orderings by changes in the oxygen content have been illustrated with $LaBaMn_2O_{5+\delta}$ as an example. The changes in the oxygen stoichiometry controls the valence state of Mn and the hybridization interaction between Mn and O. Hence, a reduction in oxygen stoichiometry narrows the bandwidth and consequently decreases the double-exchange interactions at the expense of the competing superexchange interactions. Consequently the ferromagnetic state becomes destabilized relative to the antiferromagnetic state with localized spin, charge, and orbital order as well as Jahn-Teller-type electron-lattice coupling. Therefore by adjusting the oxygen stoichiometry in manganites one can convert the insulating antiferromagnetic charge- and/or orbital-ordered state into a metallic ferromagnetic state.

The authors are grateful to the Research Council of Norway for financial support. Part of these calculations were carried out on the Norwegian supercomputer facilities.

*Electronic address: vidya.ravindran@kjemi.uio.no

[1] A.J. Millis, in *Colossal Magnetoresistance Oxides*, edited by Y. Tokura (Gordon and Breach, Singapore, 2000), p. 53.

[2] J.F. Mitchell, D.N. Argyriou, and J.D. Jorgensen, in *Colossal Magnetoresistance Oxides*, edited by Y. Tokura (Gordon and Breach, Singapore, 2000), p. 1.

[3] F. Millange, V. Caignaert, B. Domengés, and B. Raveau, Chem. Mater. **10**, 1974 (1998).

[4] A. Barnabe, F. Millange, A. Maignan, M. Hervieu, G. Van Tendeloo, and B. Raveau, Chem. Mater. **10**, 252 (1998).

[5] V. Caignaert, F. Millange, B. Domengés, and B. Raveau, Chem. Mater. **11**, 930 (1999).

[6] J.M. Wills, O. Eriksson, M. Alouani, and D.L. Price, in *Electronic Structure and Physical Properties of Materials*, edited by H. Dreysse (Springer, Berlin, 2000), p. 148.

[7] O.K. Andersen, Phys. Rev. B **12**, 3060 (1975).

[8] J.P. Perdew, S. Burke, and M. Ernzerhof, Phys. Rev. Lett. **77**, 3865 (1996).

[9] P. Blaha, K. Schwarz, and J. Luitz, computer code WIEN97 (Vienna University of Technology, Vienna, 1997) [an improved and updated Unix version of the original copyrighted code published by P. Blaha, K. Schwarz, P.I. Sorantin, and S.B. Trickey, Comput. Phys. Commun. **59**, 399 (1990)].

[10] R. Vidya, P. Ravindran, A. Kjekshus, and H. Fjellvåg, Phys. Rev. B **65**, 144422 (2002).

[11] V.I. Anisimov, J. Zaanen, and O.K. Andersen, Phys. Rev. B **44**, 943 (1991).

[12] T. Nakajima (private communication).

[13] P. Ravindran, A. Kjekshus, H. Fjellvåg, A. Delin, and O. Eriksson, Phys. Rev. B **65**, 064445 (2002).